



**Low-Temperature Cross-Linking of Polyethyleneimine
Ethoxylated Using Silane Coupling Agents to Obtain Stable
Electron Injection Layers in Solution-Processed Organic
Light-Emitting Devices**

Journal:	<i>Journal of Materials Chemistry C</i>
Manuscript ID	TC-ART-03-2019-001177.R1
Article Type:	Paper
Date Submitted by the Author:	16-Apr-2019
Complete List of Authors:	Ohisa, Satoru; Yamagata University, Graduate School of Organic Materials Science; Yamagata University, Research Center for Organic Electronics; Yamagata University, Frontier Center for Organic Materials Takashima, Dai; Yamagata University, Graduate School of Organic Materials Science Chiba, Takayuki; Yamagata University, Graduate School of Organic Materials Science; Yamagata University, Research Center for Organic Electronics; Yamagata University, Frontier Center for Organic Materials Kido, Junji; Yamagata University, Graduate School of Organic Materials Science; Yamagata University, Research Center for Organic Electronics; Yamagata University, Frontier Center for Organic Materials

ARTICLE

Low-Temperature Cross-Linking of Polyethyleneimine Ethoxylated Using Silane Coupling Agents to Obtain Stable Electron Injection Layers in Solution-Processed Organic Light-Emitting Devices

Received 00th January 20xx,
Accepted 00th January 20xx

DOI: 10.1039/x0xx00000x

Satoru Ohisa,^{*a,b,c} Dai Takashima,^a Takayuki Chiba,^{a,b,c} and Junji Kido^{*a,b,c}

This study investigates low-temperature cross-linking of polyethyleneimine ethoxylated (PEIE) using four types of silane coupling agents, including trimethyl[3-(trimethoxysilyl)propyl]ammonium chloride (TTSPAC), trimethoxyphenylsilane (TMPS), trimethoxy[3-(phenylamino)propyl]silane (TPAPS) and 1,2-bis(trimethoxysilyl)ethane (BTMSE). The results of this study indicated that all the silane coupling agents reacted with PEIE at low temperatures ranging from 65°C–120°C. The reacted PEIE exhibited solvent tolerance, indicating the cross-linking of PEIE. The cross-linked PEIE films were applied to electron injection layers (EILs) in solution-processed organic light-emitting devices. The device with PEIE: TTSPAC EIL showed a shorter device lifetime than that with only PEIE EIL. The shorter device lifetimes were attributed to the migration of chloride anions of TTSPAC. Conversely, the devices with PEIE: TMPS, TPAPS and BTMSE EILs, which did not contain mobile ions, had longer device lifetimes than that with only PEIE EIL. These results suggested that these improvements of device stability resulted from the cross-linking of PEIE.

1. Introduction

Organic light-emitting devices (OLEDs) have attracted great attention for use in displays and next generation lighting systems.¹ Currently, OLED displays are widely used for smart phones and large-sized TVs all over the world. Conversely, lower costs and longer device lifetimes are necessary for lighting applications compared with display applications. Hence, further development of high-performance OLEDs and low-cost device production processes are in high demand. Solution-processing has been investigated and employed to reduce manufacturing costs below those associated with conventional evaporation processing because solution-processing enables high-speed and large-area device production process.^{2–6} However, device performance of solution-processed OLEDs is lower than devices using evaporation-processed OLEDs. To improve the performance of devices using OLEDs, the development of efficient solution-processable electron injection layer (EIL) materials are highly desirable because EILs facilitate electron injection from cathode to organic functional layer.^{7–26} To date, various EIL materials, such as alkali-metals,⁷ alkali-metal salts,^{8,11} metal-complexes,^{9,12,22,23} organic salts,^{20,25,26} amine compounds^{15,16,18,21,25} and metal oxides^{19,24} have been developed. Among these, polyethyleneimine and

polyethyleneimine ethoxylated (PEIE) have attracted significant attention as highly-efficient EILs based on the study results reported by Zhou et al.¹⁶ However, these materials have demonstrated a low level of stability. For example, the glass transition temperature (T_g) of PEIE is -24°C .^{22,25} This low thermal stability is fatal because it can negatively affect the device lifetime. Therefore, increasing the stability of these materials is strongly desired.

Cross-linking is one method to improve the stability of organic materials. Stoltz et al. reported on the cross-linking of amino-functionalized polyfluorene (PFN) using 1,8-diiodooctane.²⁷ The cross-linked PFN was applied as an EIL in OLEDs, and the device with the cross-linked PFN demonstrated a lower driving voltage and higher driving stability compared with a device with PFN that was not cross-linked. To improve device stability in solar cells, the cross-linking of materials has been extensively studied. The primary cross-linking functional groups that have been investigated include bromine, vinyl, acrylate, azide and oxetane groups.^{28,29} Silane coupling agents (SCAs) have also attracted significant attention for use as low-temperature processable cross-linkers, which can be used at several tens of $^\circ\text{C}$, to connect materials with hydroxyl groups.^{30–35} The SCAs contain alkoxy groups bound to silicon atoms and react with the hydroxyl groups of materials via a condensation reaction. Bai et al. reported the enhancement in the stability and efficiency of perovskite solar cells using fullerene functionalized by cross-linkable silanes.³¹ Li et al. reported efficiency and stability improvements of inverted polymer solar cells using silane coupler-modified indium tin oxide (ITO) electrodes.³² As indicated in these reports, the introduction of SCAs are useful for improving the stability of solar cells. Consequently, we hypothesized that the stability of OLEDs with PEIE EILs, which contains terminal hydroxyl groups, would also be improved by the introduction of SCAs.

^a Graduate School of Organic Materials Science, Yamagata University, 4-3-16 Jonan, Yonezawa, Yamagata, Japan.

^b Research Center for Organic Electronics, Yamagata University, 4-3-16 Jonan, Yonezawa, Yamagata, Japan.

^c Frontier Center for Organic Materials, Yamagata University, 4-3-16 Jonan, Yonezawa, Yamagata, Japan.

*E-mail: s.ohisa@yz.yamagata-u.ac.jp, kid@yz.yamagata-u.ac.jp

† Electronic supplementary information (ESI) available. See DOI: 10.1039/x0xx00000x

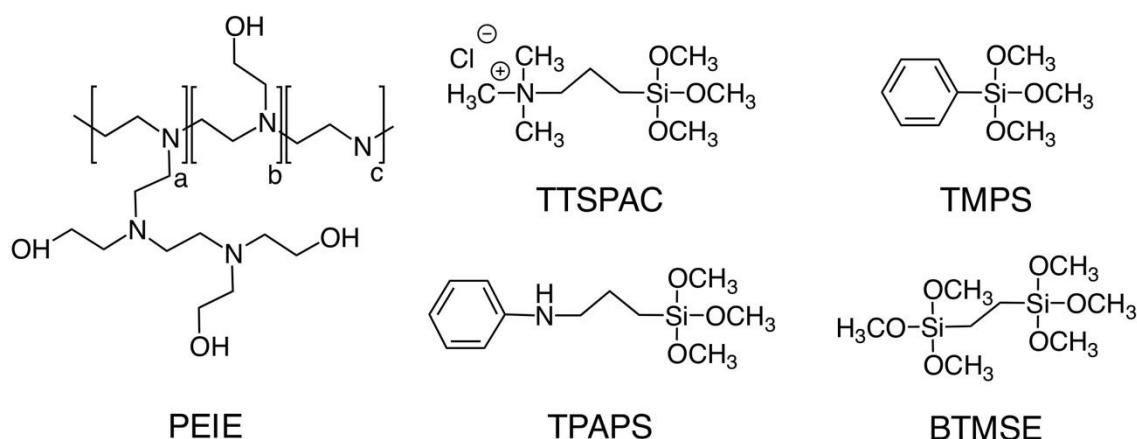


Figure 1. Chemical structures of PEIE and four types of silane coupling agents, TTSPAC, TMPS, TPAPS and BTMSE.

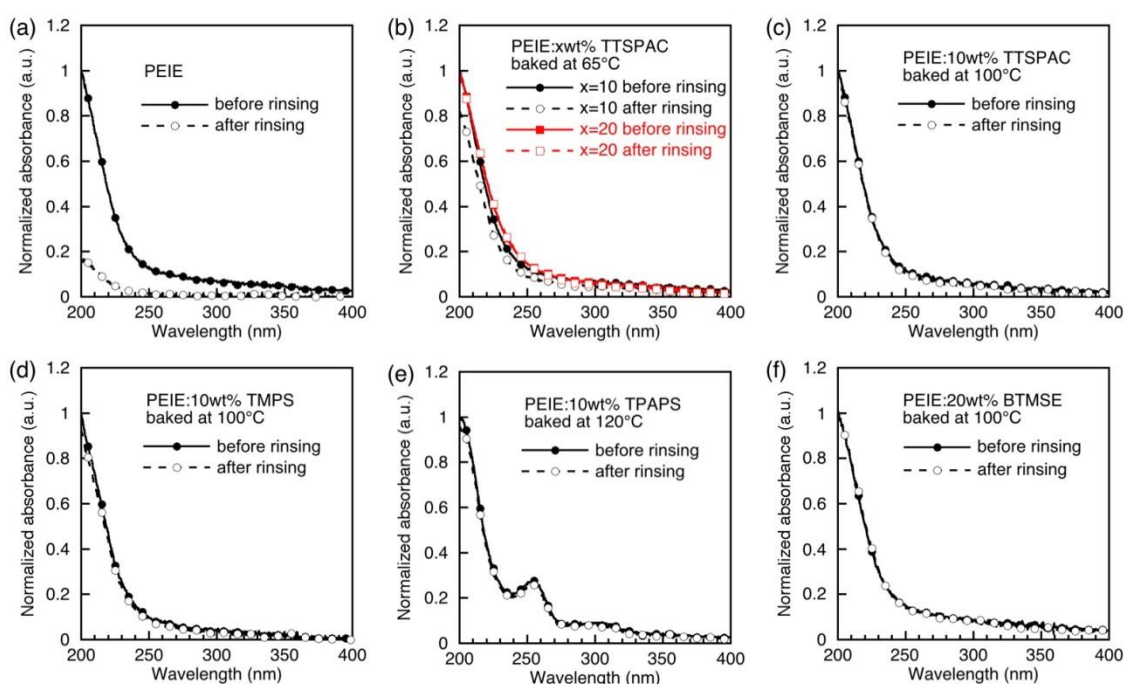


Figure 2. Solvent tolerance test results of (a) PEIE, (b) PEIE: 10 wt% and 20 wt% TTSPAC baked at 65°C, (c) PEIE: 10 wt% TTSPAC baked at 100°C, (d) PEIE: 10 wt% TMPS, (e) PEIE: 10 wt% TPAPS and (f) PEIE: 20 wt% BTMSE films.

In this work, we report the cross-linking of PEIE using four types of SCAs, which was evaluated by solvent rinsing test and attenuated total reflection-Fourier transform infrared spectroscopy (ATR-FTIR). Finally, the cross-linked PEIE films were used as EILs in solution-processed OLEDs.

2. Results and Discussion

The chemical structures of PEIE and SCAs used in this work are shown in **Figure 1**. In this study, we present the results of experiments using four types of SCAs, including trimethyl[3-(trimethoxysilyl)propyl]ammonium chloride (TTSPAC), trimethoxyphenylsilane (TMPS), trimethoxy[3-(phenylamino)propyl]silane (TPAPS) and 1,2-bis(trimethoxysilyl)ethane (BTMSE). These materials have trimethoxy groups bound to silicon atoms. The solvent tolerance

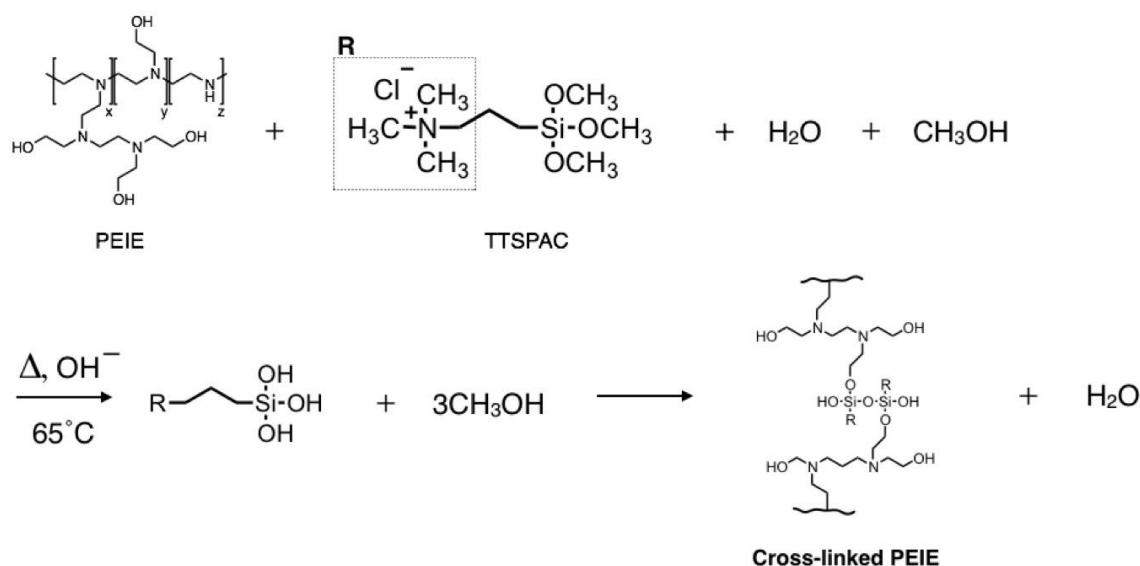


Figure 3. The proposed reaction scheme between PEIE and SCAs.

of a PEIE film to 1-butanol (BuOH) was tested by rinsing it with BuOH. The PEIE film was prepared on a quartz substrate using the spin-coating method. A BuOH droplet was placed on the PEIE film and spin-rinsed. Ultraviolet–visible (UV–vis) absorption spectra of the film were measured before and after rinsing. **Figure 2** shows the solvent rinsing test results. After rinsing, the absorbance of PEIE significantly decreased compared to its absorbance before rinsing, which indicated that PEIE is dissolved in BuOH (**Figure 2(a)**). TTSPAC was then mixed with PEIE at 10 wt% and 20 wt% ratios. PEIE: 10 wt% and 20 wt% TTSPAC films were baked at 65°C for 10 min, and these films were rinsed with BuOH. After rinsing, the PEIE: 10 wt% TTSPAC film showed an approximate 20% decrease in absorbance at 200 nm in the UV–vis spectra (**Figure 2(b)**). In contrast, the PEIE: 20 wt% TTSPAC film showed no decrease in absorbance. To investigate the effect of temperature on the cross-linking reaction, a second 10 wt% TTSPAC film was prepared and baked at 100°C for 10 min. After rinsing, the film displayed no decrease in absorbance (**Figure 2(c)**), indicating that baking it at 100°C was effective with respect to the insolubilization of PEIE associated with cross-linking. Thereafter, 10 wt% TMPS, 10 wt% TPAPS and 20 wt% BTMSE were mixed with PEIE films and baked at 100°C, 120°C and 100°C for 10 min, respectively. After rinsing with BuOH, these films showed no decrease in absorbance, indicating that the PEIE films were insolubilized by these SCAs (**Figure 2(d)–(f)**). All the agents reacted with the PEIE at low temperatures from 65°C–120°C. Hence, this process is applicable to device fabrication on flexible plastic substrates.

The cross-linking of PEIE by the SCAs was analysed by ATR–FTIR spectroscopy. Samples were formed by casting of PEIE,

the SCAs and PEIE: SCAs on Si substrates and baked at 100°C. First, the spectra of PEIE, TTSPAC, TMPS, TPAPS and BTMSE were measured. The spectra region from 700–2000 cm^{-1} are shown in **Figure S1**. PEIE displayed multiple peaks in this region. For example, the peaks at 1030 cm^{-1} and 1450 cm^{-1} were likely attributed to C–O and C–N bonds, respectively. TTSPAC, TMPS, TPAPS and BTMSE also showed multiple peaks in this region. Among them, the peaks at 1070 cm^{-1} and 1200 cm^{-1} were commonly observed except for TMPS. These two peaks could be attributed to the Si–O–Si group generated by the cross-linking reaction.³⁶ These peak positions can be influenced by the type of substituent groups connected to the Si atoms. TMPS has a Si atom bound to a phenyl group. Conversely, the others have Si atoms bound to alkyl groups. Based on these results, the peaks were likely associated with the shifting of a Si–O–Si group due to the existence of the phenyl group in TMPS, and these were not observed at the same peak positions as the others. **Figure S1** also shows the spectra of the PEIE mixed with 30 wt% SCAs. These spectra showed some peaks that were not observed in the spectra of only PEIE and each of the SCAs, indicating the creation of different types of chemical bonds. These results were likely indicative of the reaction between PEIE and the SCAs.

As an example, the proposed reaction scheme between PEIE and TTSPAC is shown in **Figure 3**.³⁷ First, the SCAs hydrolyse with the hydrolysis reaction requiring water molecules. In this study, PEIE aqueous solution was used and diluted with methanol to obtain diluted solutions. Hence, the PEIE solutions mixed with SCAs contained a small amount of water molecules. Moreover, the PEIE solution is basic and the basicity can promote the hydrolysis reaction. The

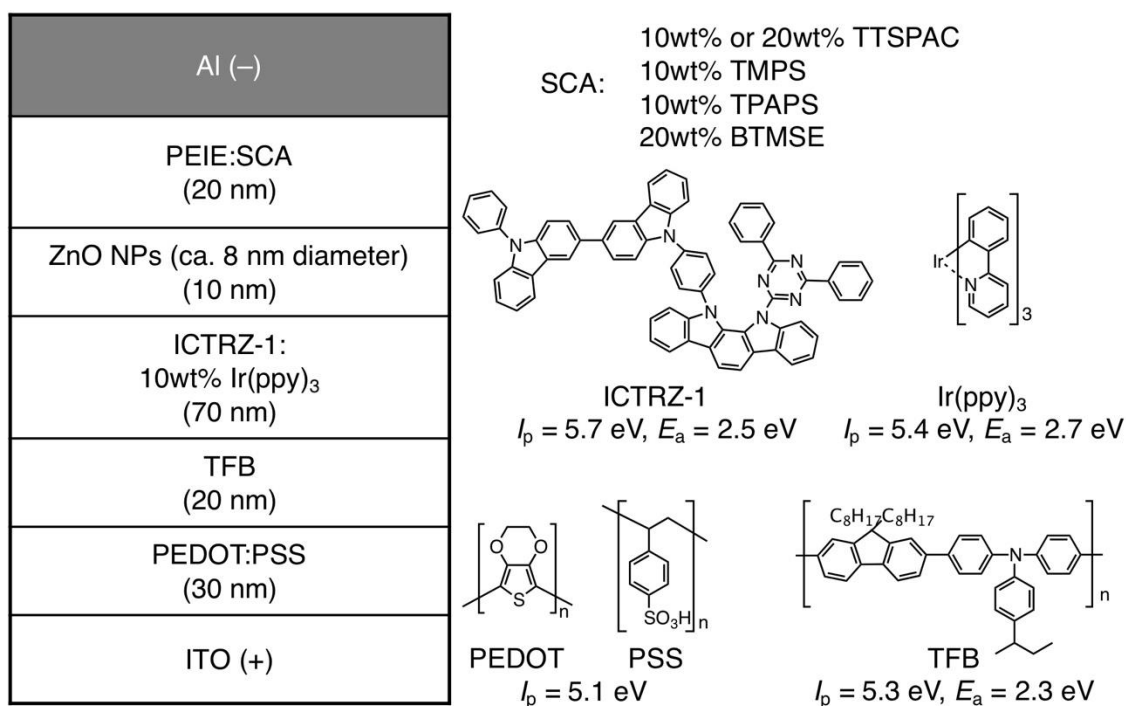


Figure 4. Organic light-emitting device structure, chemical structures used for the devices and their optoelectronic properties.

condensation reaction then progressed between the terminal hydroxyl groups of PEIE and the hydroxyl groups of the SCAs under basic condition, and as a result, the PEIE polymers were cross-linked and insolubilized.

Devices with a structure of ITO (130 nm)/poly(3,4-ethylenedioxy-thiophene):poly(4-styrenesulfonate) (PEDOT:PSS) (30 nm)/poly(9,9-dioctyl-fluorene-co-N-(4-butylphenyl)-diphenylamine) (TFB) (20 nm)/bis(phenylcarbazol)-diphenyltriazine-indolocarbazole-units containing a host material referred to as ICTRZ-1:10 wt% tris(2-phenylpyridinato)iridium(III) (Ir(ppy)₃) (70 nm)/ZnO nanoparticles (NPs) (10 nm)/EIL (20 nm)/Al (100 nm) were fabricated. Here, PEDOT:PSS, TFB, and ICTRZ-1:Ir(ppy)₃, were hole-injection layer, hole-transporting layer, and light-emissive layer (EML), respectively. The EML is hydrophobic, whereas the EILs are hydrophilic. It was difficult to form the EILs on the EILs by solution-processing. Hence, hydrophilic ZnO NPs were inserted between the EML and EILs for improvement of wettability of EILs on the EML. However, ZnO has large WF of 4.2 eV, resulting in large electron injection barrier between the EML and ZnO. On the other hand, ZnO NP film has many interspaces. During spin-coating, PEIE and the SCAs got to the ICTRZ-1: 10 wt% Ir(ppy)₃ light emission layer/ZnO NP interface.^{16,25,39} These components formed electric dipole moments at the interface causing WF shift of the ZnO NPs, facilitating electron injection from the ZnO NPs to the light

emission layer. Hence, ZnO NPs/EILs functioned as bilayer EILs. First, PEIE and PEIE: 10 wt% and 20 wt% TTSPAC were applied as the EILs. The device structure, chemical structures, ionization potentials (I_p s) and electron affinities (E_a s) of these materials are shown in **Figure 4**.^{16,19,25,38} Except for the Al cathode layer, all the layers were formed by spin coating followed by thermal baking. The spin-coated EIL films were baked for 10 min at 65°C for PEIE, and PEIE: 10wt% and 20wt% TTSPAC films. **Figures 5(a)–(c) and Figure S2** show the current density (J)–voltage (V), luminance (L)– V , external quantum efficiency (EQE)– J , current efficiency– J , power efficiency– J characteristics and EL spectra, the characteristics at 1 cd/m², 100 cd/m², and 1000 cd/m² are summarized in **Table S1**. At 1000 cd/m², the driving voltages and EQEs were 3.91 V and 9.4% for PEIE, 3.96 V and 8.6% for PEIE: 10 wt% TTSPAC, and 4.05 V and 9.7% for PEIE: 20 wt% TTSPAC, respectively. The devices with PEIE: TTSPAC showed similar driving voltages and EQE values compared with that of devices with only PEIE. Driving stabilities of the devices were evaluated at a constant current density of 5.0 mA/cm², corresponding to initial luminances of 1767 cd/m² for PEIE, 1669 cd/m² for PEIE: 10 wt% TTSPAC and 1707 cd/m² for PEIE:20 wt% TTSPAC, respectively. **Figure 5(d)** shows plots of relative luminances–driving voltages–driving time. The device with PEIE: 10 wt% TTSPAC exhibited a slightly shorter half-life of 21.0 h compared to that with only PEIE (22.3 h). Conversely, the device with

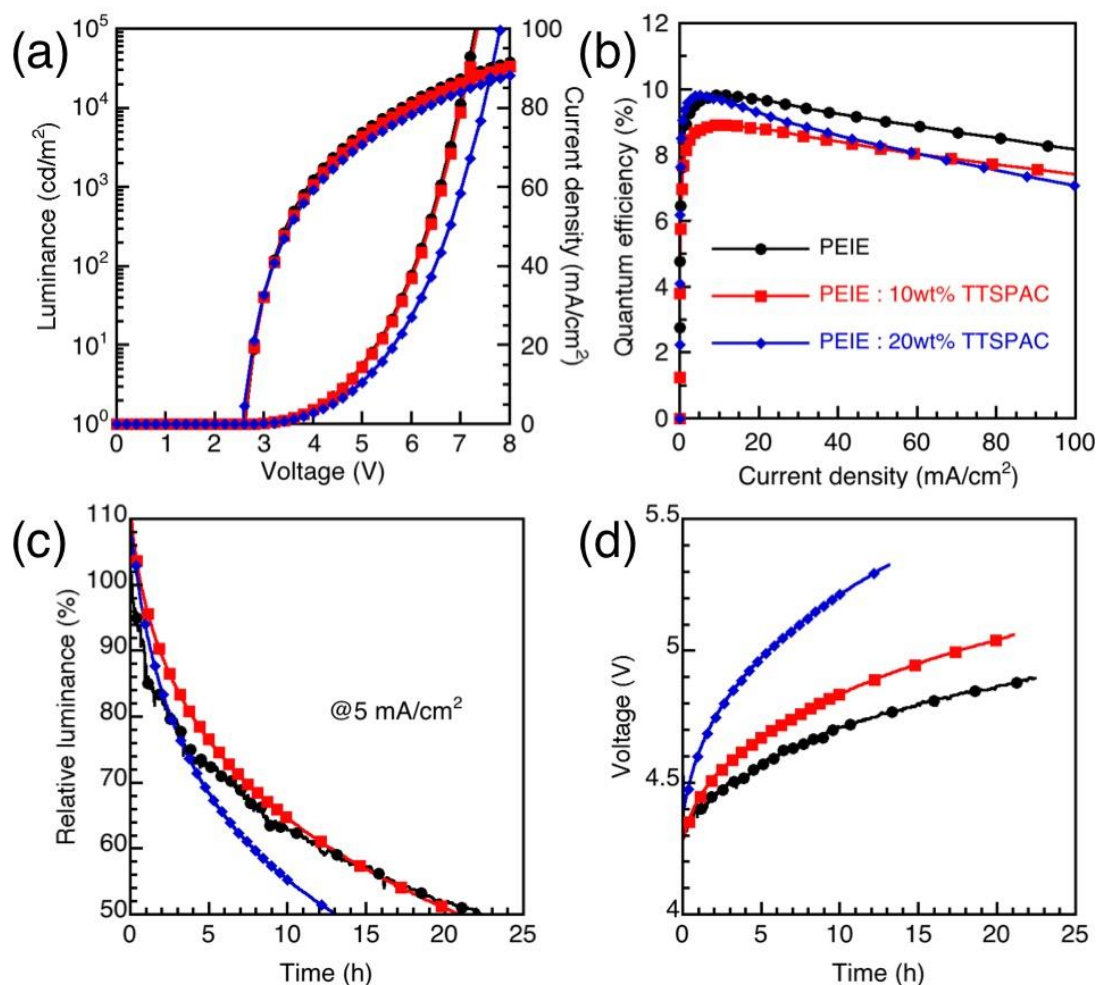


Figure 5. Characteristics of devices with PEIE, PEIE: 10 wt% TTSPAC and PEIE: 20 wt% TTSPAC EILs. (a) Current density (J)–voltage (V)–luminance, (b) external quantum efficiency– J characteristics, (c) Relative luminance–driving time (T) and (d) driving voltage– T curves.

PEIE: 20wt% TTSPAC showed a significantly shorter half-life (13.0 h) than the others. In the voltage–driving time plots, the increase in the driving voltages at 10 h was in the order PEIE < PEIE: 10 wt% TTSPAC < PEIE: 20 wt% TTSPAC. Larger amounts of TTSPAC shortened the device lifetimes. It is known that the lifetime of light-emitting electrochemical cells containing mobile ions is short due to ion migration.⁴⁰ Hence, the short lifetime was attributed to the electromigration of mobile Cl^- anions of TTSPAC under the influence of an electric field.

Finally, devices with PEIE: 10 wt% TMPS, PEIE: 10 wt% TPAPS and PEIE: 20 wt% BTMSE were fabricated. These mixed SCAs do not have mobile ions. For reference, the device with PEIE was also fabricated. The PEIE spin-coated EIL films were baked at 100°C for 10 min, and the PEIE: 10 wt% TMPS, PEIE: 10 wt%

TPAPS and PEIE: 20 wt% BTMSE films were baked at 120°C for 10 min. These SCAs were cross-linked under these baking conditions. **Figures 6(a)–(c)** and **Figure S3** show the J – V – L , EQE– J , current efficiency– J , power efficiency– J characteristics and EL spectra, and the characteristics at 1 cd/m^2 , 100 cd/m^2 , and 1000 cd/m^2 are summarized in **Table S2**. At 1000 cd/m^2 , the driving voltages and EQE values were 3.92 V and 8.9% for PEIE, 4.04 V and 9.7% for PEIE: 10 wt% TMPS, 4.22 V and 9.7% for PEIE: 10 wt% TPAPS and 4.11 V and 8.4% for PEIE: 20 wt% BTMSE, respectively. The devices with SCAs exhibited slightly higher driving voltages than that with only PEIE. With respect to device efficiency, the devices with PEIE: TMPS and PEIE: TPAPS showed higher EQEs than that with only PEIE. Conversely, the device with PEIE: BTMSE had a lower EQE than

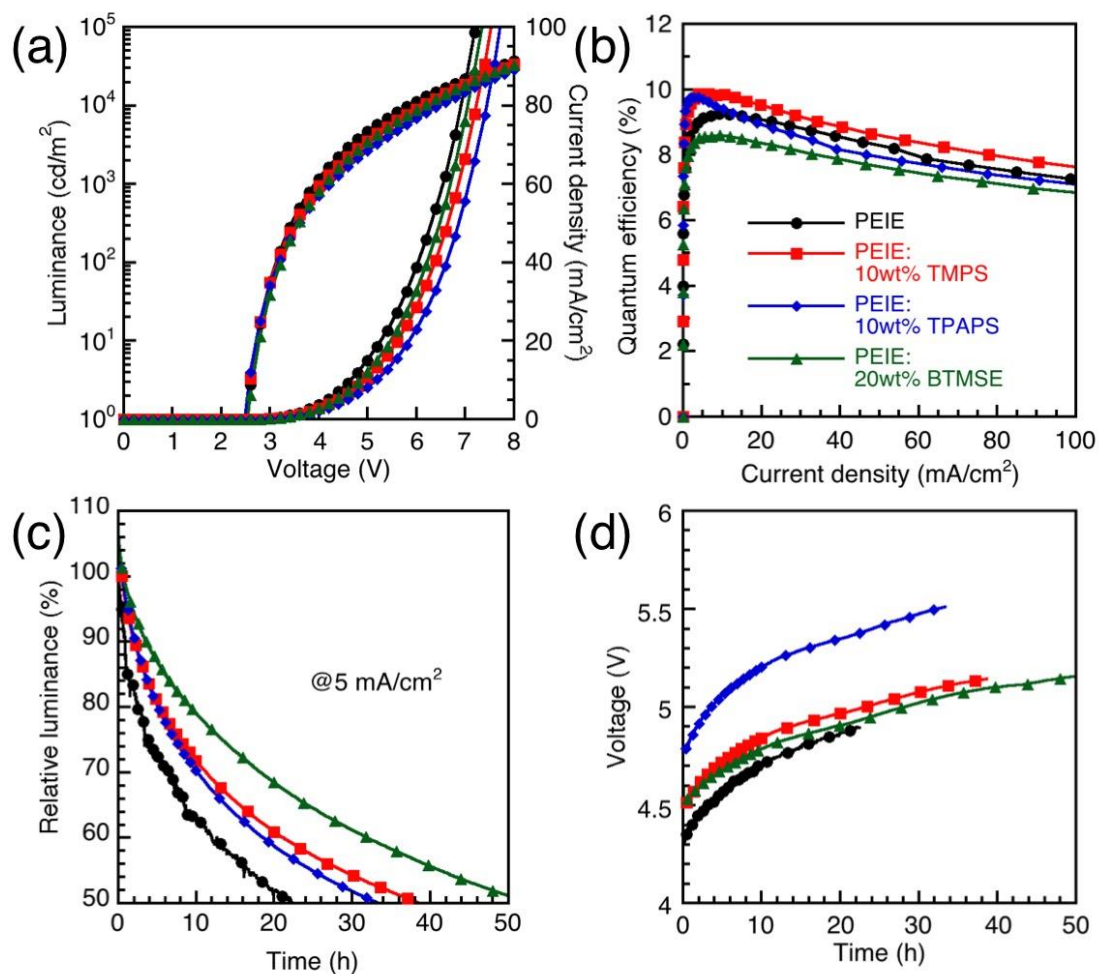


Figure 6. Characteristics of devices with PEIE, PEIE: 10 wt% TMPS, PEIE: 10 wt% TPAPS and PEIE: 20 wt% BTMSE EILs. (a) Current density (J)-voltage (V)-luminance, (b) external quantum efficiency- J characteristics, (c) Relative luminance-driving time (T) and (d) driving voltage- T curves.

that with only PEIE. PEIE has tertiary amine functional group with high basicity and it contributes to formation of electric permanent dipole at the EML/ZnO interface. On the other hand, SCAs do not have amine functional groups except TPAPS. Hence, we consider that SCAs do not contribute to the formation of electric permanent dipole at the interface, and can deteriorate the electron injection capability. In TPAPS, the amine functional group is connected to a bulky phenyl group. We considered that the bulky phenyl group inhibited the electric dipole formation by TPAPS. In addition, the generated product from PEIE:SCAs include insulating SiO₂ group. Thus, addition of SCAs can cause increase of device driving voltages. The driving stability of the devices was evaluated at a constant current density of 5.0 mA/cm², which corresponded to the initial luminances of 1767 cd/m² for PEIE, 1992 cd/m² for PEIE: 10 wt% TMPS, 1834 cd/m² for PEIE: 10 wt% TPAPS and 1730 cd/m² for PEIE: 20 wt% BTMSE, respectively. **Figure 6(d)** shows plots of relative luminance–driving voltages–driving time. These devices showed half-life's of 22.3 h for PEIE, 38.7 h for PEIE: 10 wt% TMPS, 33.3 h for PEIE:10 wt% TPAPS and 52.9 h for PEIE: 20 wt% BTMSE, respectively. In the voltage–driving time plots, the increase in the driving voltages at 10 h was in the order PEIE: 20 wt% BTMSE < PEIE: 10 wt% TMPS < PEIE < PEIE: 10 wt% TPAPS. Unlike the device with PEIE: TTSPAC containing mobile ions, the devices with SCAs, which do not contain mobile ions, exhibited longer lifetimes than that with only PEIE. Among them, the device with PEIE: 20 wt% BTMSE exhibited a half-life of about 2.5 times as long as the device with only PEIE. The devices with PEIE: 10 wt% TMPS and PEIE: 20 wt% BTMSE also displayed smaller increases in the driving voltages compared with that with only PEIE. PEIE has a glass transition temperature of −24°C, which is below room temperature. During device operation, PEIE can flow within the device, resulting in changes of the device structure after long-time device operation. Such changes of device structures give significant impacts to the device characteristics. The cross-linking can suppress the flow of PEIE within the device and contribute to improvement of device stability. Moreover, it is noteworthy that the device with PEIE baked at 100°C showed near the same characteristics and half-life as the device with PEIE baked at 65°C shown in **Figure 5**. Moreover, the T_g of the underlayer material ICTRZ-1 is 198°C,³⁸ which is greatly higher than the cross-linking temperatures in this work. Hence, we think that the difference in the cross-linking temperature among the SCAs did not give significant impacts on the devices characteristics, and believe that these improvements in the device stability were a result of the cross-linking of PEIE.

3. Conclusions

In this study, we succeeded in the low-temperature cross-linking and insolubilization of PEIE using four types of SCAs, which was supported by the results of our solvent tolerance tests and FTIR experiments. The cross-linked PEIE films were applied as EILs in solution-processed OLEDs. The device with PEIE: TTSPAC containing mobile ions exhibited shorter device lifetimes than that of the device with only PEIE. Conversely, the devices with PEIE: TMPS, TPAPS and BTMSE showed longer device lifetimes than the device with only PEIE. These improvements in device stability were attributed to the improvements of PEIE stability by cross-linking. These cross-linked PEIE films would be applicable in flexible organic

electronic devices owing to their low-temperature processing requirements. We believe the results in this work will be useful in the further development of high value-added devices, such as flexible displays, lighting systems and other flexible applications.

4. Experimental

4.1. Materials

PEIE (product No. 306185) was purchased from Sigma-Aldrich, Inc. The SCAs were purchased from Tokyo Chemical Industry Co., Ltd. PEDOT: PSS (Clevios P VP CH 8000) was purchased from Heraeus Materials Technology. TFB was purchased from American Dye Source, Inc. Ir(ppy)₃ was purchased from CHEMIPRO KASEI KAISHA, LTD. These products and materials were used as received without further purification or modification. ICTRZ-1 was synthesized according to the established procedure.³⁸ ZnO NPs were synthesized according to the established procedure.^{19,38}

4.2. General procedures

UV–vis spectra were measured using a Shimadzu UV-3150 UV–vis–NIR spectrophotometer. FTIR spectra were measured using a Shimadzu IR Prestige-21 Fourier transform spectrophotometer. The samples analysed by FTIR were fabricated by casting onto Si substrates followed by baking. For device fabrication, glass substrates with ITO electrodes were sequentially cleaned by scrub washing using a neutral detergent dissolved in ultrapure water and rinsed in ultrapure water using an ultrasonic bath sonicator before dry-cleaning using a UV-ozone cleaner. The PEDOT: PSS was spin-coated onto the substrates in air, followed by thermal baking at 200°C for 10 min. The substrates were then transferred into a N₂-purged glove box. TFB dissolved in *p*-xylene was spin-coated onto PEDOT: PSS, followed by thermal baking at 200°C for 60 min. ICTRZ-1: 10 wt% Ir(ppy)₃ dissolved in tetrahydrofuran was spin-coated onto TFB, followed by thermal baking at 100°C for 10 min. ZnO NPs alcohol solution was spin-coated onto ICTRZ-1: 10 wt% Ir(ppy)₃, followed by thermal baking at 100°C for 10 min. The PEIE dissolved in methanol was spin-coated onto the ZnO NPs layers followed by thermal baking at 65°C or 100°C for 10 min. The PEIE: SCAs dissolved in methanol was spin-coated onto the ZnO NPs layers followed by thermal baking at 65°C for PEIE: TTSPAC, or baked at 120°C for PEIE: TMPS, TPAPS and BTMSE for 10 min. Subsequently, the substrates were transferred to a vacuum chamber, and Al cathodes were deposited using a shadow mask with patterned openings. The emitting area of the devices was 2 × 2 mm. *J–V–L* characteristics were measured using a current source meter (Keithley 2400) and a luminance meter (Konica Minolta CS-200). EL spectra were measured using a photonic multichannel analyser (Hamamatsu PMA-11). Quantum efficiencies were calculated on the basis of the Lambertian assumption.

Conflicts of interest

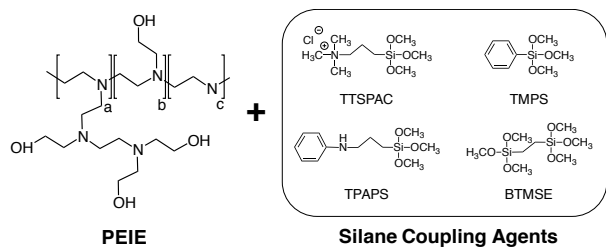
There are no conflicts to declare.

Acknowledgements

We would like to thank “the Centre of Innovation (COI) Program” of Japan Science and Technology Agency (JST) for financial support.

Notes and references

1. H. Sasabe and J. Kido, *J. Mater. Chem. C*, 2013, **1**, 1699-1707.
2. C. D. Müller, A. Falcou, N. Reckefuss, M. Rojahn, V. Wiederhirn, P. Rudati, H. Frohne, O. Nuyken, H. Becker and K. Meerholz, *Nature*, 2003, **421**, 829-833.
3. L. Duan, L. Hou, T.-W. Lee, J. Qiao, D. Zhang, G. Dong, L. Wang and Y. Qiu, *J. Mater. Chem.*, 2010, **20**, 6392-6407.
4. C. Zhong, C. Duan, F. Huang, H. Wu and Y. Cao, *Chem. Mater.*, 2011, **23**, 326-340.
5. N. Aizawa, Y.-J. Pu, M. Watanabe, T. Chiba, K. Ideta, N. Toyota, M. Igarashi, Y. Suzuri, H. Sasabe and J. Kido, *Nat. Commun.*, 2014, **5**, 5756.
6. K. S. Yook and J. Y. Lee, *Adv. Mater.*, 2014, **26**, 4218-4233.
7. J. Kido, K. Nagai and Y. Okamoto, *IEEE Transactions on Electron Devices*, 1993, **40**, 1342-1344.
8. L. S. Hung, C. W. Tang and M. G. Mason, *Appl. Phys. Lett.*, 1997, **70**, 152-154.
9. J. Endo, T. Matsumoto and J. Kido, *Ext. Abstr. 9th Int. Workshop on Inorganic & Organic Electroluminescence*, 1998, 57.
10. J. Kido and T. Matsumoto, *Appl. Phys. Lett.*, 1998, **73**, 2866-2868.
11. Q. T. Le, L. Yan, Y. Gao, M. G. Mason, D. J. Giesen and C. W. Tang, *J. Appl. Phys.*, 2000, **87**, 375-379.
12. J. Endo, T. Matsumoto and J. Kido, *J. J. Appl. Phys.*, 2002, **41**, L800-L803.
13. F. Huang, H. Wu, D. Wang, W. Yang and Y. Cao, *Chem. Mater.*, 2004, **16**, 708-716.
14. J. Y. Lee, *J. Ind. Eng. Chem.*, 2008, **14**, 676-678.
15. T. Xiong, F. Wang, X. Qiao and D. Ma, *Appl. Phys. Lett.*, 2008, **93**, 123310.
16. Y. Zhou, C. Fuentes-Hernandez, J. Shim, J. Meyer, A. J. Giordano, H. Li, P. Winget, T. Papadopoulos, H. Cheun, J. Kim, M. Fenoll, A. Dindar, W. Haske, E. Najafabadi, T. M. Khan, H. Sojoudi, S. Barlow, S. Graham, J. L. Bredas, S. R. Marder, A. Kahn and B. Kippelen, *Science*, 2012, **336**, 327-332.
17. T. Chiba, Y.-J. Pu and J. Kido, *J. Mater. Chem. C*, 2015, **3**, 11567-11576.
18. B. R. Lee, S. Lee, J. H. Park, E. D. Jung, J. C. Yu, Y. S. Nam, J. Heo, J. Y. Kim, B. S. Kim and M. H. Song, *Adv. Mater.*, 2015, **27**, 3553-3559.
19. Y.-J. Pu, N. Morishita, T. Chiba, S. Ohisa, M. Igarashi, A. Masuhara and J. Kido, *ACS Appl. Mater. Interfaces*, 2015, **7**, 25373-25377.
20. S. Ohisa, Y.-J. Pu and J. Kido, *J. Mater. Chem. C*, 2016, **4**, 6713-6719.
21. S. Stolz, M. Petzoldt, S. Duck, M. Sendner, U. H. Bunz, U. Lemmer, M. Hamburger and G. Hernandez-Sosa, *ACS Appl. Mater. Interfaces*, 2016, **8**, 12959-12967.
22. T. Chiba, Y.-J. Pu, T. Ide, S. Ohisa, H. Fukuda, T. Hikichi, D. Takashima, T. Takahashi, S. Kawata and J. Kido, *ACS Appl. Mater. Interfaces*, 2017, **9**, 18113-18119.
23. S. Ohisa, T. Karasawa, Y. Watanabe, T. Ohsawa, Y.-J. Pu, T. Koganezawa, H. Sasabe and J. Kido, *ACS Appl. Mater. Interfaces*, 2017, **9**, 40541-40548.
24. S. Ohisa, T. Hikichi, Y. J. Pu, T. Chiba and J. Kido, *ACS Appl. Mater. Interfaces*, 2018, **10**, 27885-27893.
25. S. Ohisa, T. Kato, T. Takahashi, M. Suzuki, Y. Hayashi, T. Koganezawa, C. R. McNeill, T. Chiba, Y.-J. Pu and J. Kido, *ACS Appl. Mater. Interfaces*, 2018, **10**, 17318-17326.
26. S. Sato, S. Ohisa, Y. Hayashi, R. Sato, D. Yokoyama, T. Kato, M. Suzuki, T. Chiba, Y. J. Pu and J. Kido, *Adv. Mater.*, 2018, DOI: 10.1002/adma.201705915, 1705915.
27. S. Stolz, M. Petzoldt, N. Kotadiya, T. Rodlmeier, R. Eckstein, J. Freudenberg, U. H. F. Bunz, U. Lemmer, E. Mankel, M. Hamburger and G. Hernandez-Sosa, *J. Mater. Chem. C*, 2016, **4**, 11150-11156.
28. G. Wantz, L. Derue, O. Dautel, A. Rivaton, P. Hudhomme and C. Dagron-Lartigau, *Polym. Int.*, 2014, **63**, 1346-1361.
29. F.-J. Kahle, C. Saller, A. Köhler and P. Strohriegel, *Adv. Energy Mater.*, 2017, **7**, 1700306.
30. D. Song, H. An, J. H. Lee, J. Lee, H. Choi, I. S. Park, J. M. Kim and Y. S. Kang, *ACS Appl. Mater. Interfaces*, 2014, **6**, 12422-12428.
31. Y. Bai, Q. Dong, Y. Shao, Y. Deng, Q. Wang, L. Shen, D. Wang, W. Wei and J. Huang, *Nat. Commun.*, 2016, **7**.
32. Y. Liu, N. Aghdassi, Q. Wang, S. Duhm, Y. Zhou and B. Song, *Org. Electron.*, 2016, **35**, 6-11.
33. P. Fu, X. Guo, S. Wang, Y. Ye and C. Li, *ACS Appl. Mater. Interfaces*, 2017, **9**, 13390-13395.
34. Z. Li, Y. Liu, K. Zhang, Z. Wang, P. Huang, D. Li, Y. Zhou and B. Song, *Langmuir*, 2017, **33**, 8679-8685.
35. R. Matthews, E. Glasser, S. C. Sprawls, R. H. French, T. J. Peshek, E. Pentzer and I. T. Martin, *ACS Appl. Mater. Interfaces*, 2017, **9**, 17620-17628.
36. H.-J. Jeon, S.-C. Yi and S.-G. Oh, *Biomaterials*, 2003, **24**, 4921-4928.
37. Jalil Morshedian and P. M. Hoseinpour, *Iran. Polym. J.*, 2009, **18**, 103-128.
38. S. Ohisa, T. Takahashi, M. Igarashi, H. Fukuda, T. Hikichi, R. Komatsu, E. Ueki, Y.-J. Pu, T. Chiba and J. Kido, *Adv. Funct. Mater.*, 2019, DOI: 10.1002/adfm.201808022, 1808022.
39. J. J. Kang, T. Y. Yang, Y. K. Lan, W. R. Wu, C. J. Su, S. C. Weng, N. L. Yamada, A. C. Su and U. S. Jeng, *Small*, 2018, **14**, 1704310.
40. S. B. Meier, D. Tordera, A. Pertegás, C. Roldán-Carmona, E. Ortí and H. J. Bolink, *Mater. Today*, 2014, **17**, 217-223



Cross-linking for Improvement of PEIE Stability

Cross-linking of polyethylenimine ethoxylated using silane coupling agent improved stability of organic light-emitting devices.